Available online at www.sciencedirect.com
ScienceDirect
Palaeogeography, Palaeoclimatology, Palaeoecology 260 (2008) 389–404
PALAEO
www.elsevier.com/locate/palaeo

The magnetic properties of loess and paleosol samples from the Chinese Loess Plateau spanning the last 22 million years

Qingzhen Hao [a,b], Frank Oldfield [b,*], Jan Bloemendal [b], Zhengtang Guo [a]

[a] *Institute of Geology and Geophysics, Chinese Academy of Sciences, Beijing 100029, China*
[b] *Department of Geography, University of Liverpool, Liverpool L69 7ZT, UK*

Received 7 July 2007; received in revised form 8 November 2007; accepted 26 November 2007

Abstract

Magnetic measurements (susceptibility, isothermal and anhysteretic remanence, and quotients derived from these) are presented for a suite of loess and paleosol samples from sites on the Chinese Loess Plateau. The three sites, Xifeng, Dongwan and Qinan (QA-I), together span most of the last 22 million years. The results provide the first multi-parameter magnetic measurements from pre-Pleistocene loess/paleosol sequences that began accumulation in the early Miocene. Mass specific measurements have been corrected for carbonate concentrations which peak in the loess layers and range up to 57%. All the magnetic properties recorded indicate variability on both orbital and supra-orbital timescales. The changing magnetic properties allow the record to be divided into a sequence of eight sample groups that broadly parallel the main supra-orbital changes in magnetic susceptibility. The pre-Pleistocene parts of the record include intervals (mainly late Miocene and Pliocene) during which loess as well as paleosol layers are characterized by high values for properties such as frequency dependent susceptibility (χ_{fd}), usually associated with strong weathering. Most of the Miocene record prior to 8.5 Ma, with the exception of a brief interval from ca. 14.4 to 15.9 Ma, shows reduced values for indicators of pedogenic ferrimagnetic concentrations in both the loess and paleosol layers, as well as a low amplitude of variability between loess and paleosol values. The palaeoenvironmental implications of this part of the sequence are unclear since they hinge on the type of model of pedogenic magnetic mineral formation adopted. High-field remanence measurements indicate that the coercivity of the antiferromagnetic minerals represented declined progressively throughout the whole period in both the loess and the paleosol samples, though there is no unambiguous evidence for long-term diagenetic alteration of the magnetic properties on timescales beyond the orbital ones that drive the loess/paleosol alternations. The present results suggest caution in applying existing climofunctions based on magnetic susceptibility to deposits spanning the whole of the last 22 Ma.

Keywords: Loess; Environmental magnetism; Neogene; Palaeoenvironment; China

1. Introduction

Recent studies have shown that loess deposition in the western part of the Chinese Loess Plateau (Fig. 1) began at least 22 million years (Ma) ago (Guo et al., 2002). Confirmation of an aeolian origin for the deposits in the pre-Pleistocene sections comes from studies of granulometry (Qiao et al., 2006), quartz morphology and quartz grain size (Liu et al., 2006) and malacological analysis (Li et al., 2006a,b). The chronology of loess accumulation has been established through analysis of fossil micro-mammalian remains and magnetostratigraphy (Guo et al., 2002; Hao and Guo, 2004). In the case of the oldest, Miocene section (QA-I), the chronology and stratigraphic integrity of most of the section have also been confirmed by a comparison of the detailed magnetostratigraphy with that at a parallel site 30 km distant (Liu et al., 2005).

Measurements of magnetic susceptibility of the pre-Pleistocene sites show that, as at the classic Quaternary sections, alternations between episodes dominated by the deposition of loess and intervening periods of soil formation have occurred during most if not all of the whole period of accumulation (Guo et al., 2002; Hao and Guo, 2004; see also Fig. 2). According to the chronology as currently defined, these oscillations have

* Corresponding author. Fax: +44 151 794 2866.
E-mail address: oldfield.f@gmail.com (F. Oldfield).

0031-0182/$ - see front matter © 2008 Elsevier B.V. All rights reserved.
doi:10.1016/j.palaeo.2007.11.010

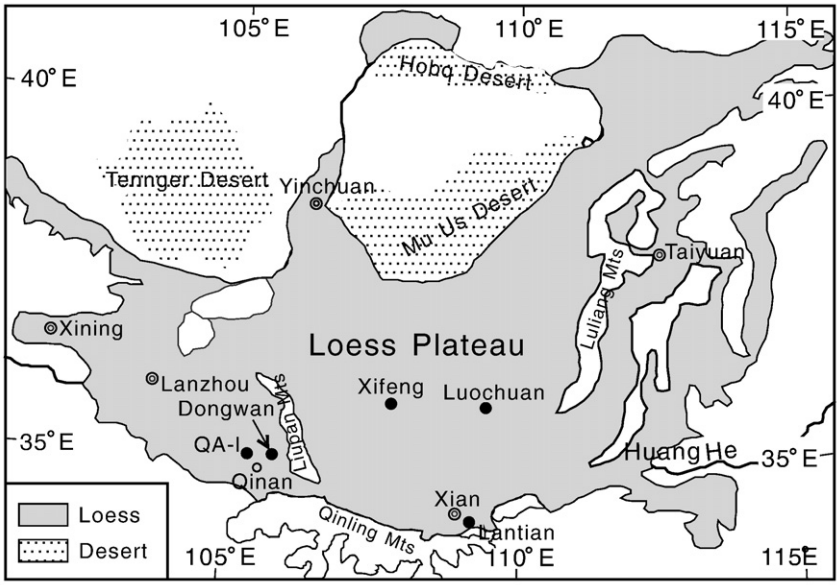

Fig. 1. Location map showing the Loess Plateau and the location of the site mentioned.

occurred on orbital timescales (e.g. Guo et al., 2004a,b). Superimposed on these orbital frequency alternations are clear indications of longer timescale variability. These are recognizable in the visual characteristics of the loess and the interbedded paleosols, by differences in the mean susceptibility values of both loess and paleosols and by changes in the amplitude of variability in susceptibility values between adjacent paleosol and loess layers. There are also differences in the chemical characteristics of the paleosols, and in their granulometry (e.g. Guo et al., 2002).

Soil iron oxide mineralogy is sensitive to climate and can rapidly be characterized using rock magnetic techniques (e.g. Thompson and Oldfield, 1986; Evans and Heller, 2003). Since Heller and Liu (1984) first recognized that the low-field magnetic susceptibility variations of the Chinese loess–soil sequences could be closely correlated with deep-sea oxygen isotope records, one of the focuses in the loess study has been concentrated on variations in magnetic mineralogy, magnetic grain size, and their implication for palaeoclimate, as reviewed by Heller and Evans (1995), Evans and Heller (2001) and Liu et al. (2007b). Magnetic susceptibility has long been regarded as a proxy for East Asian summer monsoon intensity (e.g., An et al., 1991). Some susceptibility-based climofunctions have also been proposed to quantitatively estimate paleoprecipitation (e.g. Heller et al., 1993; Maher et al., 1994; Liu et al., 1995; Han et al., 1996). All these previous magnetic investigations have been limited to the Quaternary aeolian deposits; investigations of pre-Quaternary loess sequences have been relatively few (Liu et al., 2003). The rock magnetic properties, mineralogy and the recorded climate history of the Neogene aeolian deposits on the western Chinese Loess Plateau have not been previously studied. The present study of long-term changes of magnetic properties is designed to provide an initial basis for a better understanding of the relationship between the formation of soil iron oxide mineralogy and changes in the climate regimes in northern China.

In the present paper, we seek to characterize and compare the magnetic properties of both loess and paleosol samples representative of different types of loess/paleosol couplet within the whole of this time interval. In the case of the sequences from Dongwan and Qinan (Fig. 1), together spanning almost all of the period from 3.7 to 22 Ma, our results provide the first systematic, multi-parameter rock magnetic measurements from sites of long-term, pre-Pleistocene, aeolian accumulation. The present paper is a preliminary one, designed to set the scene for more detailed rock magnetic measurements and for a synthesis of palaeoenvironmental evidence linking the magnetic record to geochemical, granulometric and pollen analytical data.

2. The study sites and choice of samples

Fig. 1 locates the sites used in this study. The Xifeng site lies at 1200 m elevation in the centre of the Loess Plateau, but to the east of the Liupan Mountains and with a mean present day annual precipitation of 544 mm and a mean annual temperature of 8.5 °C. The Dongwan site, with a surface elevation of 1900 m, lies in the drier western part of the Loess Plateau. The Qinan, QA-I site lies some 30 km west of the Dongwan section and has a top elevation of 1860 m. Annual precipitation at Qinan, close to these western sites, is ca. 515 mm at the present day and the mean annual temperature is 10.4 °C. Precipitation in both the eastern and western regions occurs mainly in summer when the East Asian monsoon brings moist air inland. The pattern of spatial variability in monsoon-linked precipitation, notably the declining trend from south-east to north-west, characteristic of the present day climate, appears to have persisted during interglacial periods at least over the last 600 ka (Hao and Guo, 2005). However, during earlier Neogene times, when the Tibetan Plateau was not so high, atmospheric circulation patterns may have been

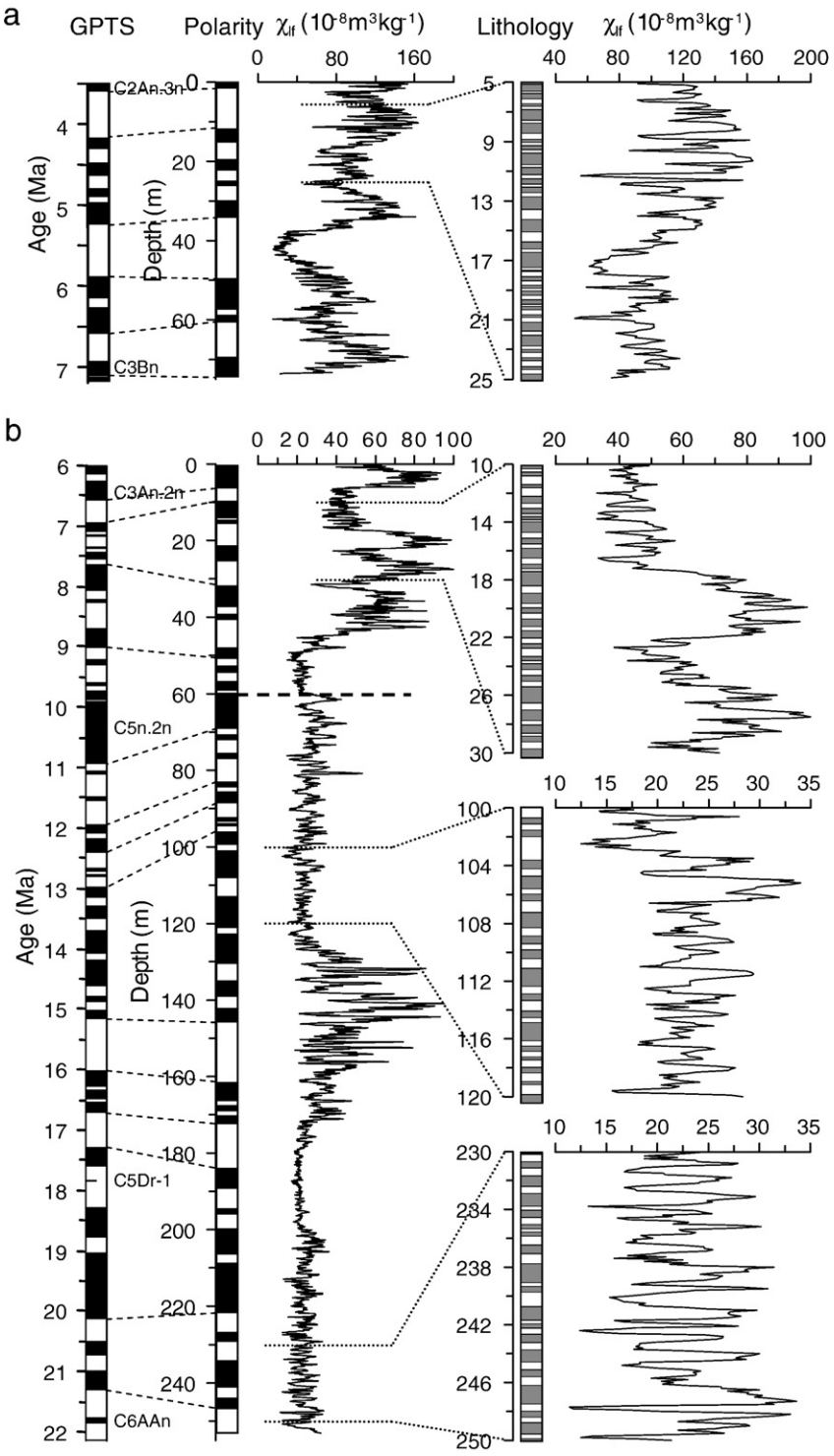

Fig. 2. Expansion of the 10 cm interval χ_{lf} measurements for selected time intervals from the Dongwan (a) and QA-I (b) sections, set alongside the lithological record of loess/paleosol alternations. In the lithological column, the grey bars indicate soil layers and the open bar, loess layers.

significantly different, with the Southwest monsoon playing a more important role.

Routine magnetic measurements were carried out on a total of 106 samples. These were selected from the three long sequences to represent some of the main variations apparent in the low frequency magnetic susceptibility (χ_{lf}) measurements that have previously been completed (Guo et al., 2002; Hao and Guo, 2004; Fig. 2).

2.1. Xifeng

Thirty alternating paleosol and loess samples from the Quaternary part of the sequence, spanning the period from S0 (Holocene) to L33 (2.55 Ma).

Six samples from the Pliocene *Hipparion* Red Earth part of the sequence between 2.6 and 3.4 Ma.

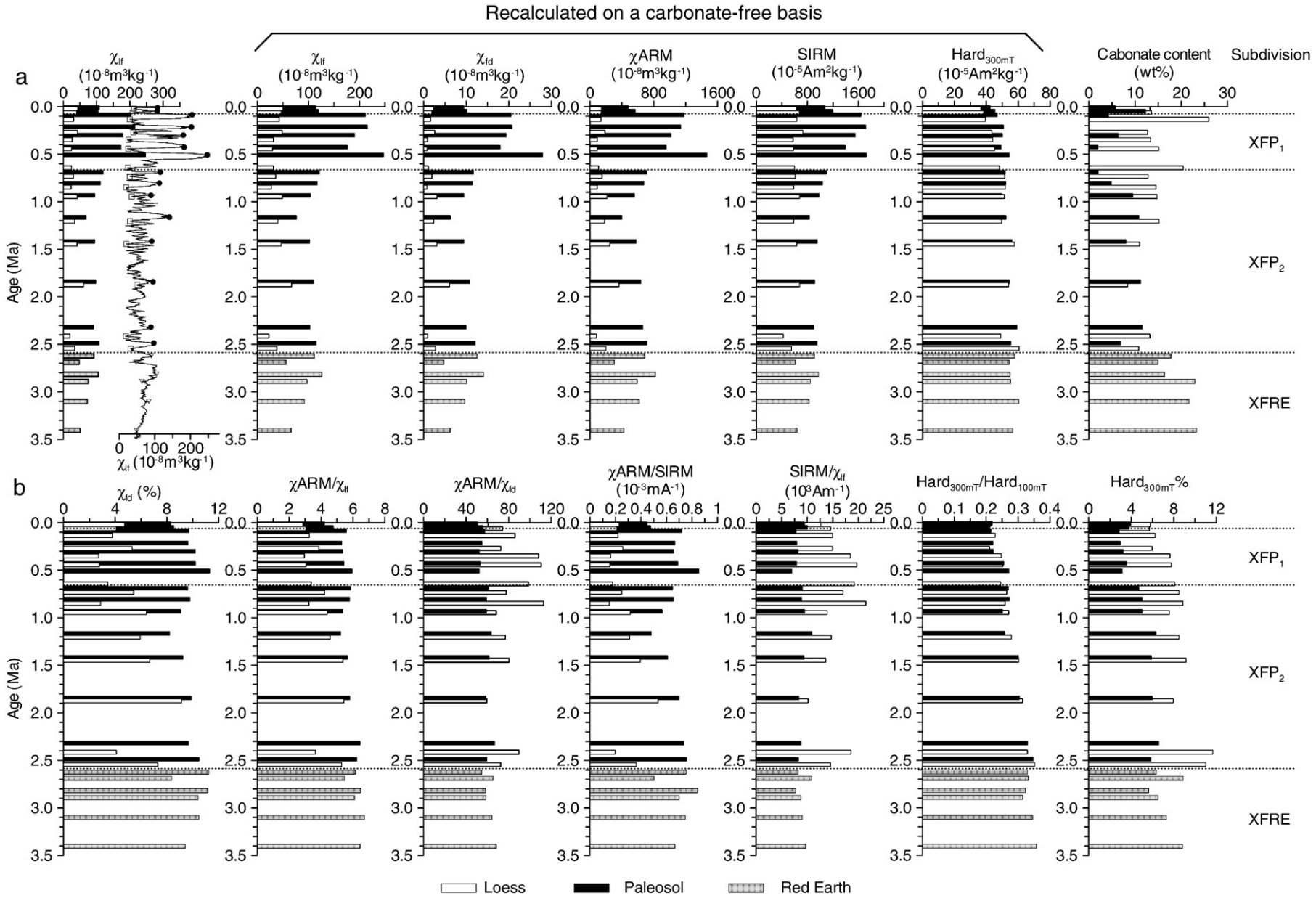

Fig. 3. The Xifeng section: selected magnetic properties and carbonate concentrations versus age. In (a), the left-hand histogram and the curve of χ_{lf} values have not been corrected for carbonate concentrations. The curve of χ_{lf} values plotted alongside the first histogram shows the trace of the χ_{lf} measurements made at 10 cm intervals. Marked on this trace are the points at which loess (open symbols) and paleosol (solid symbols) samples were taken for the full suite of routine measurements. The carbonate concentrations used in recalculating the carbonate-free values are shown on the right-hand side of the graph. (b) shows selected quotient and percentage values. In both figures, loess and paleosol samples are distinguished except in the case of the *Hipparion* Red Earth samples where such a distinction was not possible from the lithology.

2.2. Dongwan

Twenty alternating paleosol and loess samples from a 73.7 m thick late Miocene–Pliocene sequence spanning the time interval from 3.7 to 7 Ma (Hao and Guo, 2004).

2.3. Qinan (QA-I)

Fifty alternating paleosol and loess samples from a 253.1 m thick Miocene sequence spanning the time interval from 6.4 to 22 Ma (Guo et al., 2002).

3. Methods

All samples were subject to the following sequence of magnetic measurements:

Low frequency magnetic susceptibility (χ_{lf}) measured at 0.47 kHz and high frequency magnetic susceptibility (χ_{hf}), at 4.7 kHz, using a Bartington MS2 meter. The difference between the two measurements gives the frequency dependent susceptibility expressed either as a mass specific property (χ_{fd}) or as a percentage of χ_{lf} (χ_{fd}%).

Anhysteretic Remanent Magnetisation (ARM) using a DTECH demagnetizer-ARM with a peak alternating field of 100 mT and a DC biasing field of 0.1 mT. The plotted values ($\chi_{ARM}\chi_{ARM}$". Please check if appropriate.–>) have been normalized for the DC biasing field.

Saturation Isothermal Remanent Magnetisation (SIRM) using a field of 1 T generated by an MMPM5 Pulse Magnetiser.

Reverse field demagnetization of the SIRM at fields of −20 mT, −40 mT, −100 mT and −300 mT.

All remanence measurements were made using a Molspin spinner magnetometer with a noise level of 0.1×10^{-8} A m^2.

Figs. 3a, 4a and 5a plot on a mass specific basis, low-field susceptibility (χ_{lf}), SIRM, χ_{ARM} and $Hard_{300\ mT}$ (the part of the SIRM that remains un-reversed after application of a field of −300 mT). In the left-hand column of each figure, the full susceptibility profile, based on measurements at 10 cm intervals, is shown as a continuous line alongside the histograms of χ_{lf} for the samples used for multi-parameter measurements. All other histogram values are plotted on a carbonate-free basis using the carbonate concentration values plotted at the right-hand edge of each figure.

Figs. 3b, 4b and 5b plot the following quotient and percentage values: the percentage frequency dependent susceptibility (χ_{fd}%), χ_{ARM}/χ_{lf}, χ_{ARM}/χ_{fd}, χ_{ARM}/SIRM, SIRM/χ_{lf}, $IRM_{300\ mT}$ as a percentage of SIRM ($(SIRM+IRM_{-300\ mT})/(2\times SIRM)\times100\%$) and $Hard_{300\ mT}/Hard_{100\ mT}$ (roughly comparable to Liu et al. (2007a) '*L*' parameter).

The interpretation of these measurements is discussed in several earlier publications (e.g. Zheng et al., 1991; Yu and Oldfield, 1993; Chen et al., 1995; Walden et al., 1999).

4. Results

On each of the figures and for most of the analysis and discussion, loess (open bars) and paleosol layers (solid bars) are considered separately, except in the case of the Pliocene Xifeng *Hipparion* Red Earth (Red Clay) formation within which they could not be distinguished.

4.1. The Quaternary sequence from Xifeng

The upper and middle parts of Fig. 3a and b, dating from 0–2.6 Ma show the routine measurements from the Holocene and Pleistocene part of the Xifeng sequence plotted against sample age. The two uppermost paleosols are from the Holocene and an Interstadial soil above S1 which latter represents MIS 5. The greater amplitude of change between loess and paleosol samples characteristic of the susceptibility values in the part of the sequence postdating 0.6 Ma is also reflected in the SIRM and χ_{ARM} profiles. It is not so clearly marked in either the Hard IRM measurements or in the quotient and percentage values.

All of the indicators of finer magnetic grain size, χ_{ARM}, χ_{ARM}/SIRM and χ_{fd}%, peak in the paleosol samples. In the part of the sequence postdating 0.5 Ma, hard remanence measurements are higher in the paleosols than in the loess suggesting that the antiferromagnetic minerals present are partly of pedogenic origin (cf. Torrent et al., in press). The measurements are consistent in all respects with previous measurements from Xifeng and other classic sections in the central-eastern part of the Loess Plateau (e.g. Bloemendal and Liu, 2005). They therefore provide reference data for comparison with the much less studied Pliocene and Miocene sequences, though the more easterly location of the site should be born in mind.

4.2. The Xifeng Hipparion Red Earth samples

The six samples, ranging in age from 2.6–3.4 Ma, are shown in the lower parts of Fig. 3a and b. They come from the part of the sequence not demonstrably affected by reworking or groundwater (Guo et al., 2001b, 2004b) and they were not clearly distinguishable as either loess or paleosol. The values for most of the properties and quotients measured fall within the same range as those in the lower half of the Pleistocene sequence.

4.3. The Dongwan Miocene–Pliocene sequence

Throughout the sequence from 3.7–7 Ma, loess and paleosol layers are clearly distinguishable both visually and in the bulk magnetic susceptibility measurements (Fig. 4).

There is little systematic difference between χ_{lf}, SIRM, χ_{ARM} and Hard IRM values, corrected for carbonate concentrations, in the paleosols and the intervening loess samples. The values for χ_{lf}, SIRM and Hard IRM in the paleosols are within the range for the Xifeng Pleistocene samples, but χ_{ARM} values are, on average, somewhat higher. This suggests that magnetite/maghemite concentrations in the Dongwan paleosols are comparable to those in the Pleistocene paleosols at Xifeng, but are much higher in the loess layers. There is little consistent difference between adjacent loess and paleosol samples in any of the quotient values (Fig. 4b). Even the χ_{fd}% values in the loess are comparable to those in many Pleistocene paleosols and the χ_{ARM}/SIRM quotient values are mostly higher. From these

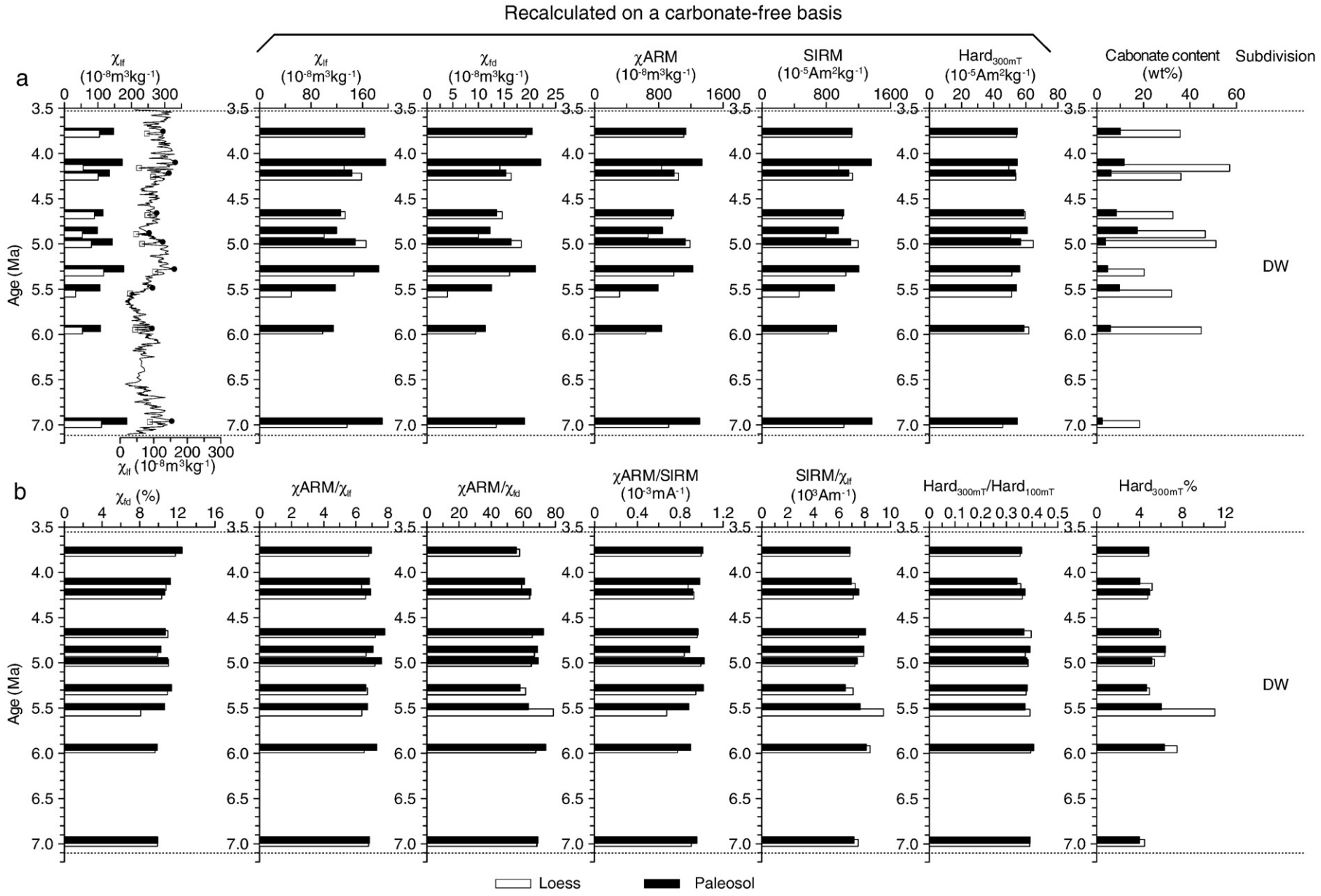

Fig. 4. The Dongwan section: selected magnetic properties and carbonate concentrations versus age. (a) is plotted as for Fig. 3(a), and (b) as for Fig. 3(b).

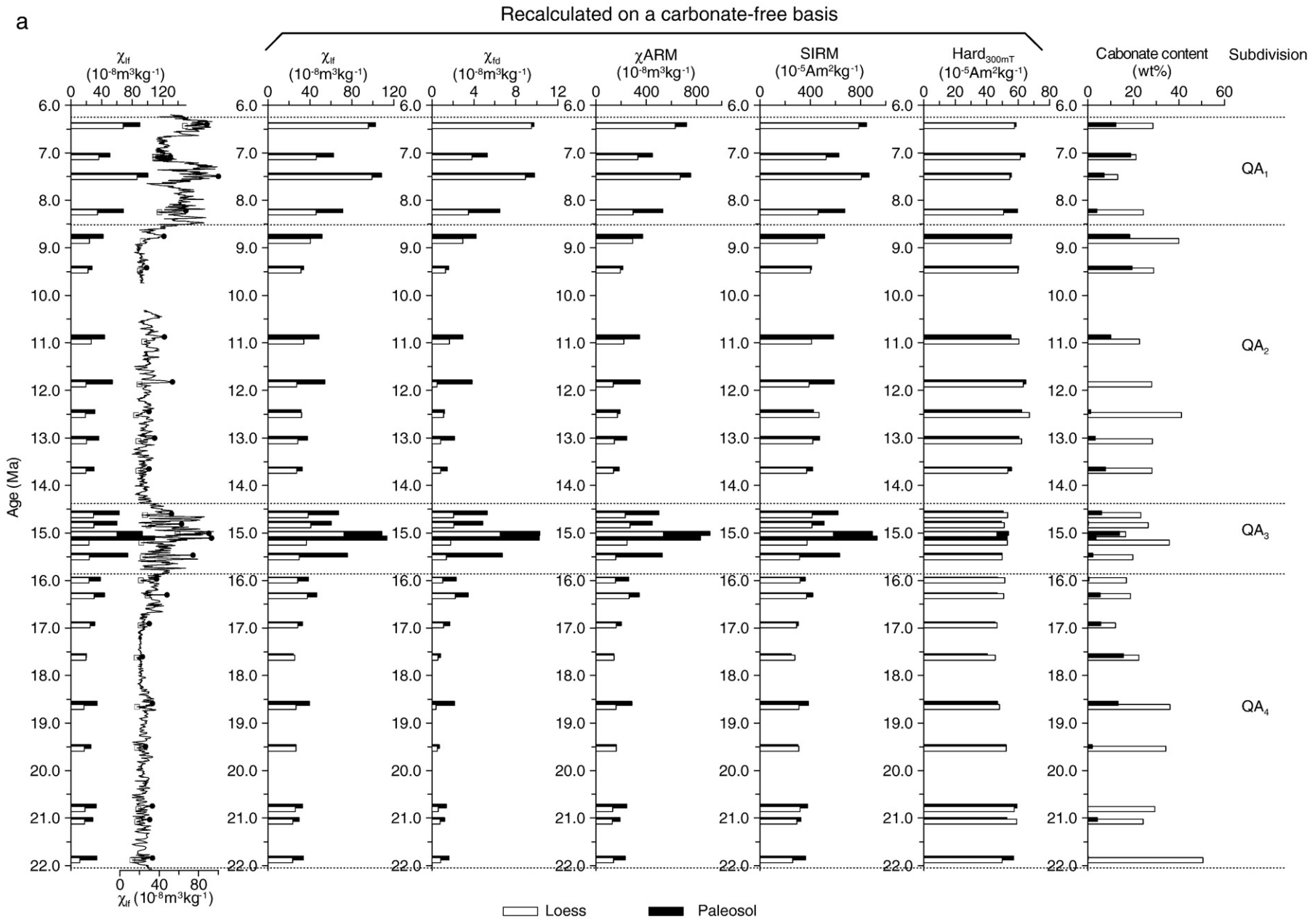

Fig. 5. The QA-I section: selected magnetic properties and carbonate concentrations versus age. (a) is plotted as for Fig. 3(a), and (b) as for Fig. 3(b).

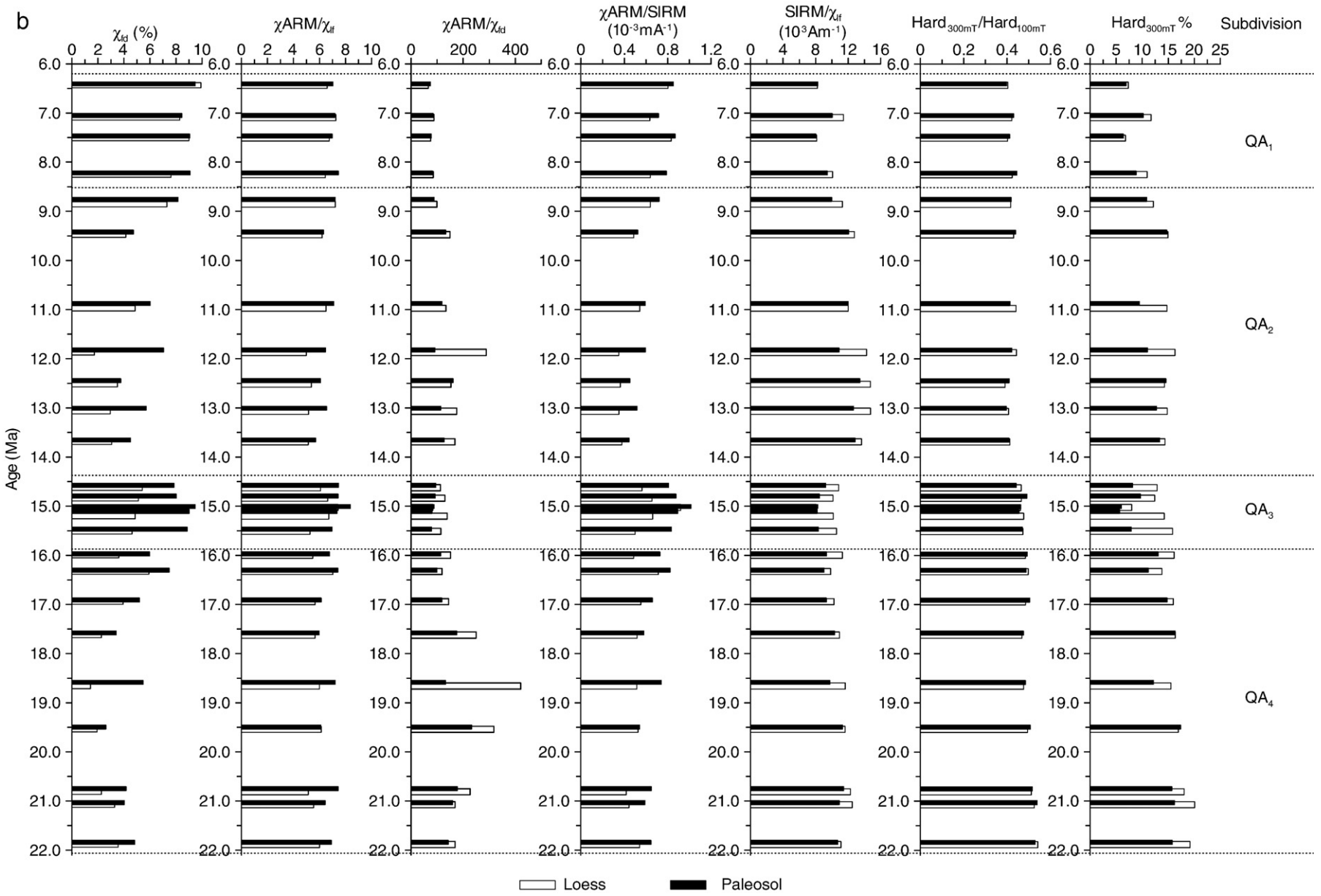

Fig. 5 (*continued*).

data, there would appear to be much less difference in the magnetic concentrations, grain size and mineral assemblages in the loess and paleosol samples from Dongwan. The inference is that pedogenesis has affected the loess layers here much more than in the Pleistocene loess. Comparison between bulk susceptibility values and the same measurements corrected for carbonate concentrations suggests that changing carbonate concentrations are largely responsible for the orbital-scale variability seen in the continuous curve of 10 cm spaced values throughout most of the sequence.

4.4. The Qinan (QA-I) Miocene sequence

The 50 samples measured from the QA-I section (Fig. 5a and b) span almost all of the sequence from 6.4–22 Ma. Samples corresponding to paleosol and loess layers can be recognized throughout the section.

χ_{lf} values are higher in the paleosols throughout the profile, though the amplitude of the difference varies significantly at different depths. However, because the samples selected are not always from the same couplet, they do not always reflect the loess/paleosol alternations in adjacent strata. Curves for SIRM, and to a lesser degree χ_{ARM}, χ_{ARM}/SIRM and χ_{fd}%, parallel those for susceptibility. In the two zones where χ_{lf} values are highest, between ca. 6.2–8.5 Ma and 14.4–15.9 Ma, all the concentration and quotient values in the paleosols are similar to those in paleosols from the lower Pleistocene sections from Xifeng. Between these depths, paleosol concentrations of all but the Hard IRM component are generally lower and all indications are that ferrimagnets, presumably pedogenic magnetite/maghemite grains, are significantly less abundant, though antiferromagnet concentrations are at least as high as in the Pleistocene paleosols. Ferrimagnetic concentrations in the loess samples are broadly similar to those in the Pleistocene loess except that after 8.5 Ma, they are consistently higher, as are the χ_{fd}% and χ_{ARM}/SIRM values. This part of the sequence includes, at the top, a zone of overlap with that from Dongwan. The susceptibility measurements do not provide detailed correlations between the two sequences, possibly because the lower part of the Dongwan section contains some evidence of reworking (Hao and Guo, 2004). Nevertheless, in both sequences where they overlap, there are similar indications of pedogenesis strongly affecting the magnetic properties of the loess. Below this in the QA-I section, the amplitude of variation between paleosol and loess layers is least where susceptibility values are lowest. Despite this, and even after correction for carbonate concentrations, parameters associated with ferrimagnetic concentrations are still generally higher in paleosols than in loess layers.

4.5. The results of the PATN analyses

From the above account it is clear that for both the loess and the paleosol samples, there are similarities and subtle

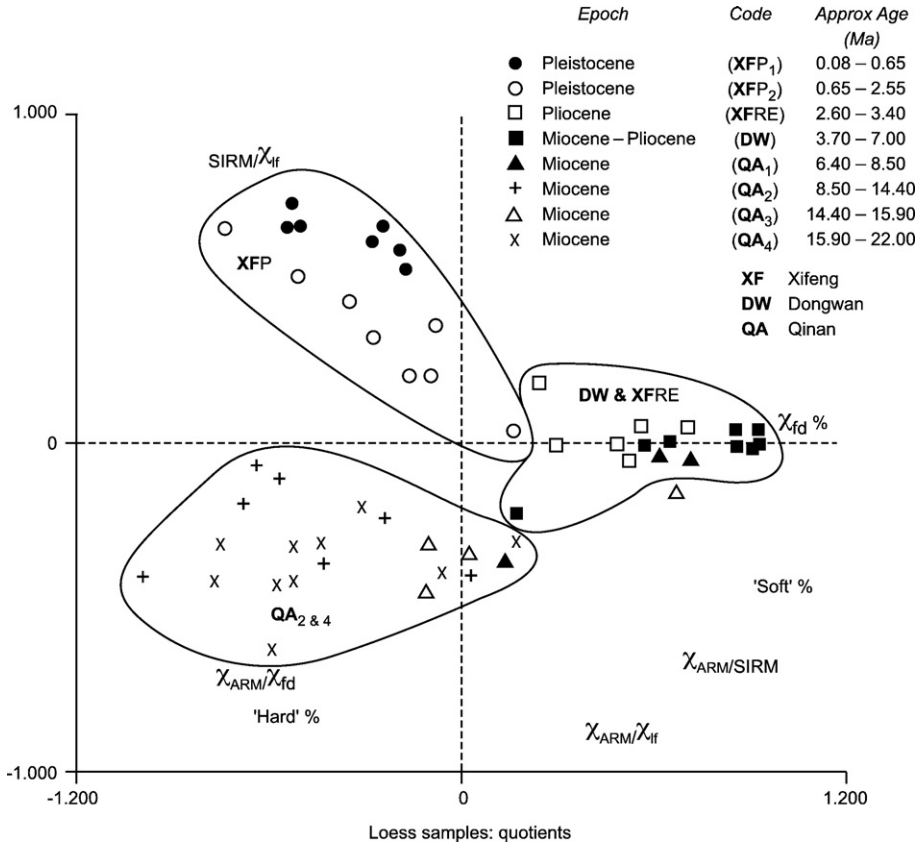

Fig. 6. Loess samples. PATN ordination plot of selected quotient and percentage values: χ_{ARM}/SIRM; χ_{ARM}/χ_{lf}; χ_{ARM}/χ_{fd}; SIRM/χ_{lf}; $IRM_{-300\ mT}$ and $IRM_{-20\ mT}$ as percentages of SIRM (HardIRM% and SoftIRM% respectively) and χ_{fd}%.

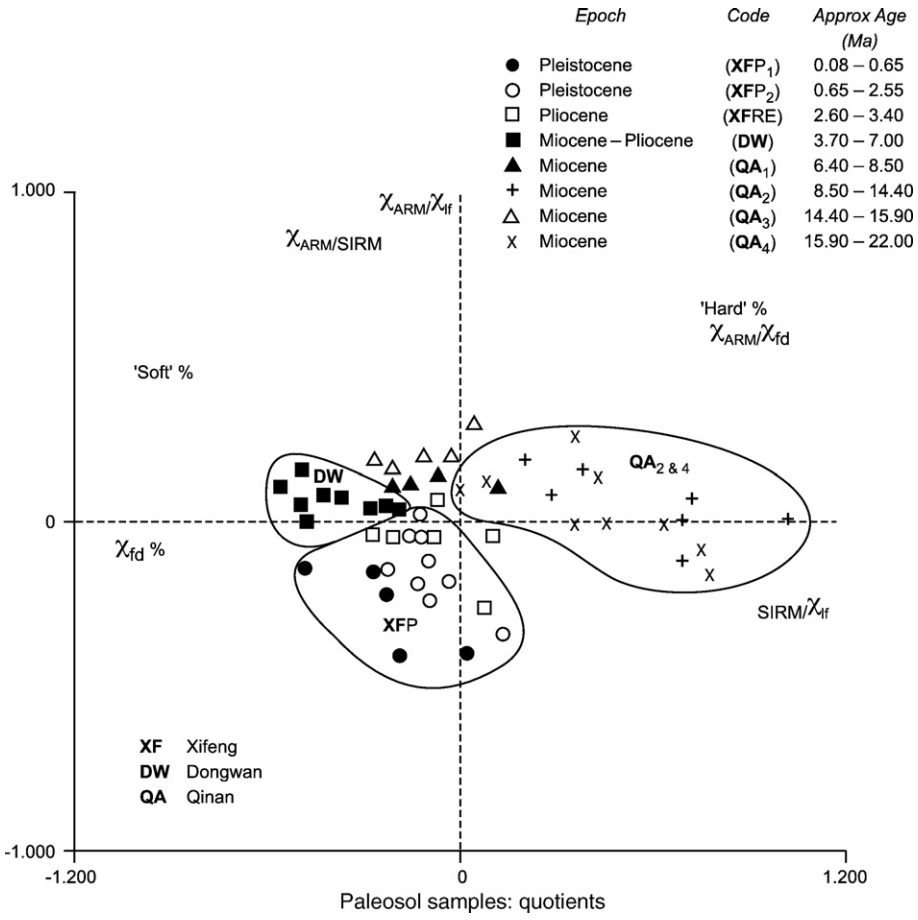

Fig. 7. Paleosol samples. PATN ordination plot of selected quotient and percentage values (as for Fig. 6).

differences between the magnetic properties of samples representing different parts of the 22 Ma period studied. In order to better characterize these for the sample set as a whole, ordination procedures were applied to a range of quotient values, using the PATN program (Belbin, 1987, 1988) previously applied successfully to rock magnetic data (Yu and Oldfield, 1993; Oldfield et al., 2003). The loess and paleosol samples were split into separate groups. The only samples common to both groups are those from the Xifeng Red Earth, since these remain unascribed. Fig. 6 plots quotient and percentage values for loess, and Fig. 7 for paleosols. In all the plots, and in most of the subsequent presentation and discussion, the sequence as a whole is divided into eight subsets of samples, as follows:

1. The Xifeng Pleistocene section (XFP_1) from S1 to L6 (MIS 13 to 5; ca. 0.08–0.65 Ma).
2. The Xifeng Pleistocene section (XFP_2) from S6 to the base (ca. 0.65–2.55 Ma).
3. The Xifeng *Hipparion* Red Earth (XFRE) (ca. 2.6–3.4 Ma).
4. The Dongwan section (DW) (ca. 3.7–7 Ma).
5. The upper part of the QA-I profile (QA_1) characterized by high χ_{lf} values (ca. 6.4–8.5 Ma).
6. The upper middle section of the QA-I profile (QA_2), characterized by lower χ_{lf} values and a low amplitude of variation in χ_{lf} between loess and paleosol layers (ca. 8.5–14.4 Ma).
7. The lower middle section of the QA-I profile (QA_3), characterized by higher χ_{lf} values in the paleosol layers (ca. 14.4–15.9 Ma).
8. The lowest section of the QA-I profile (QA_4), characterized by low χ_{lf} values and a low amplitude of variation in χ_{lf} between paleosol and loess layers (ca. 15.9–22 Ma).

In each of the PATN plots, values for the properties identified decline from the point on the plot where each is placed, along a series of planes normal to a line drawn from that point through the origin of the graph. The plots thus make it possible both to judge the extent to which the properties give similar indications of between-site and temporal variations in the sample sets, and to place subsets of samples into groups with respect to variations in the properties plotted. The program calculates the correlation coefficients between the property values and the fitted vectors for each. These are as follows:

Loess quotients and percentages (Fig. 6): $R^2 > 0.87$ except for χ_{ARM}/χ_{fd} ($R^2 = 0.62$).
Paleosol quotients and percentages (Fig. 7): $R^2 > 0.81$.

In both plots, the QA_2 and QA_4 sets are distinguished by the lowest values for χ_{fd}%. Almost all the DW samples have high values for χ_{fd}% in both plots. In the loess plot (Fig. 6), although both the QA_2 and QA_4 sets and XFP share relatively low χ_{fd}%

values, they are clearly separated by higher χ_{ARM}/χ_{fd} and Hard% values in the QA_2 and QA_4 sets and higher SIRM/χ in XFP. In the paleosol plot also (Fig. 7), higher χ_{ARM}/χ_{fd} and Hard% values distinguish QA_2 and QA_4 from XFP. A common feature of the plots is the consistency with which the magnetic properties of sample groups QA_2 and QA_4, spanning most of the time interval from 9–22 Ma, can be distinguished from the other groups.

5. Discussion

5.1. Ferrimagnetic grain size

Several of the quotients used in the present study are sensitive to ferrimagnetic grain size (cf. Maher, 1988). χ_{fd}% values are proportional to the contribution of fine viscous (FV) components to total low-field susceptibility (Liu et al., 2004b) and high values often indicate high contributions from super-paramagnetic (SP) grains (Dearing et al., 1996). χ_{ARM}/SIRM values are sensitive to the balance between stable single domain (SSD) and pseudo-single domain (PSD)+multidomain (MD) grains, with higher values for the quotient indicating dominance by the former. χ_{ARM}/χ_{lf} values are less easy to interpret without setting them alongside the other two. Banerjee et al. (1981) showed that in predominantly PSD and MD assemblages, higher values for the quotient pointed to smaller grain diameters. Conversely, Oldfield (1994), following Maher (1988), showed that provided it can be demonstrated that ferrimagnetic grains with diameters in the SSD range and finer dominate the assemblage, χ_{ARM}/χ_{lf} increases with increasing grain size. χ_{fd}% and χ_{ARM}/SIRM provide the necessary criteria for selecting samples dominated by fine grains (Oldfield, 1994), hence likely to show a positive relationship between χ_{ARM}/χ_{lf} and grain diameter. Within a group of samples selected in this way, both χ_{ARM}/χ_{fd} and χ_{ARM}/χ_{lf} are sensitive to the varying proportions of grains above or below the SP:SSD boundary and a convenient way of representing the results is on a bilogarithmic plot using these quotients as axes. Fig. 8 shows such a plot with the data from all the paleosols in the eight groups as well as the loess samples in the Dongwan, QA_1 and

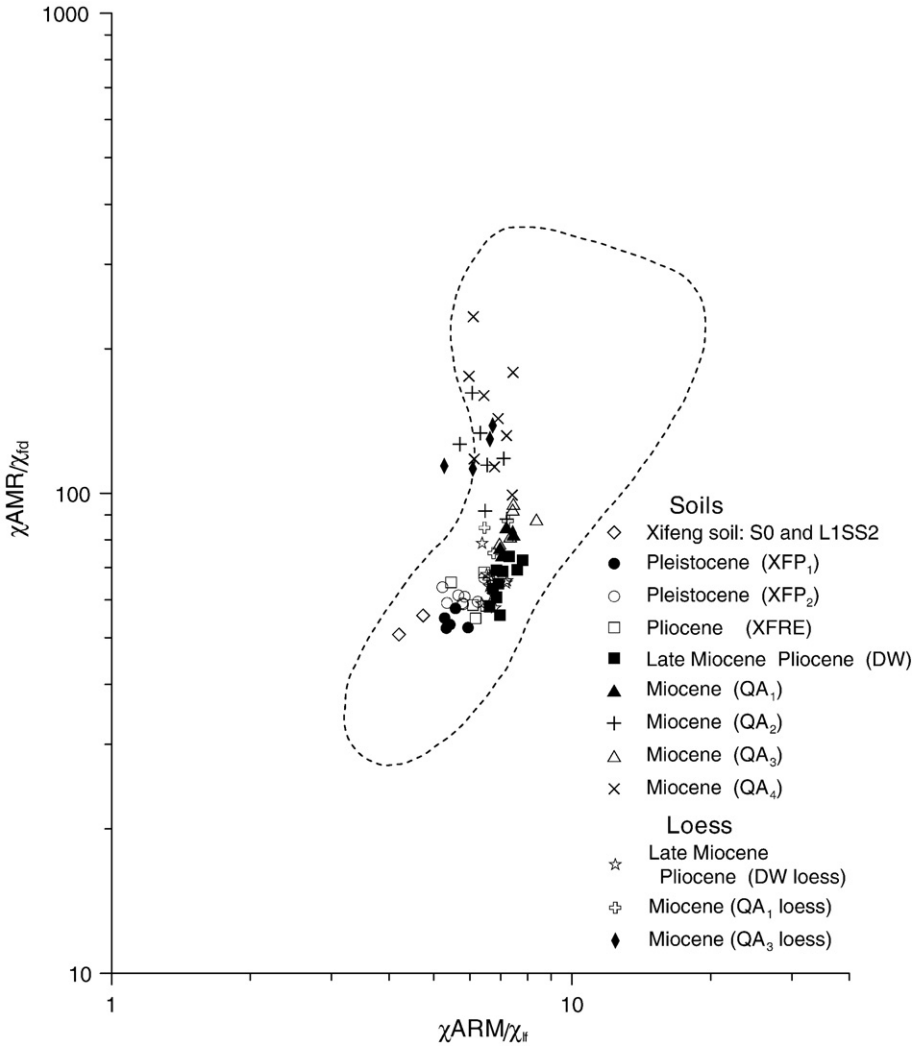

Fig. 8. Bilogarithmic plot of χ_{ARM}/χ_{fd} versus χ_{ARM}/χ_{lf}. The open envelope is taken from Oldfield (1994) as corrected in Oldfield (in press) and represents the range of values for this quotient in a variety of contemporary and fossil soils from Europe and Asia.

QA_3 sets, superimposed on the envelopes of values for magnetically enhanced soils/paleosols and for samples dominated by bacterial magnetosomes (Oldfield, 1994, in press). All the other loess sample sets have χ_{fd}% and χ_{ARM}/SIRM values that fail to meet the required criteria for unambiguous interpretation of their position on the diagram.

The samples shown in Fig. 8 all plot within the envelope typical of magnetically enhanced soils and paleosols. The values of both quotients are much too low to be influenced significantly by bacterial magnetosomes and too high to be much affected by burning, since that leads to the formation of finer grains, resulting in values consistently closer to the bottom left-hand corner of the graph (Oldfield and Crowther, 2007). The higher values of χ_{ARM}/χ_{fd} in the QA-I paleosols compared with the rest, already noted above, suggest that a higher proportion of the ferrimagnetic grains in the older material is in the SSD rather than SP size range.

In the loess samples not included in Fig. 8, it is possible that both fine grains and grains above the SSD boundary contribute to the susceptibility and soft remanence measurements. This is

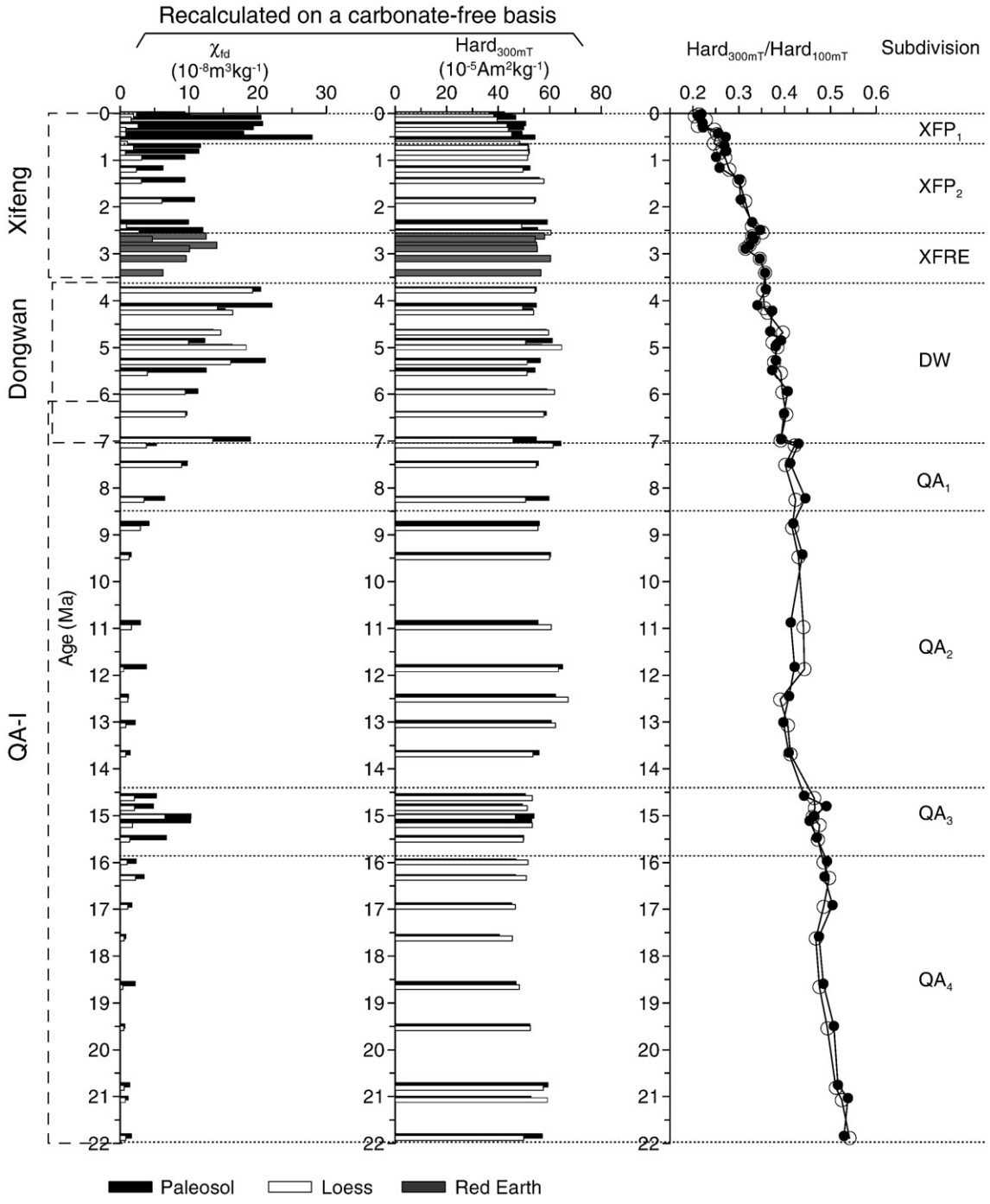

Fig. 9. χ_{fd} and $IRM_{300\ mT}$ plotted against age for the whole sequence with loess and paleosol values distinguished as in Figs. 3–5. The right-hand column shows the values for the modified '*L*' parameter (see Fig. 10), with loess and paleosol samples distinguished by open and solid symbols respectively.

suggested by particle size based measurements on loess from sites both on the western (Chen et al., 1995) and central (Zheng et al., 1991) parts of the Loess Plateau.

These results accord with the view that the magnetic mineral assemblage in all the paleosols, and in the late Miocene and early Pliocene loess at least, includes a significant contribution from fine grained ferrimagnetic minerals. Although several earlier studies considered that the mineral in question was magnetite (e.g. Maher, 1998), recent evidence points to maghemite (Liu et al., 2004a; Torrent et al., in press) as the dominant fine grained, pedogenic, ferrimagnetic mineral. χ_{fd} is probably the best single magnetic property available for characterizing the relative abundance of this component in each of the sequences studied (Fig. 9).

5.2. Imperfect antiferromagnetic minerals

Magnetically Hard IRM, here represented as $IRM_{300\ mT}$, has often been used to approximate the contribution of canted antiferromagnetic minerals to the magnetic properties. These minerals comprise hematite and goethite. The Hard IRM parameter is strongly affected not only by variations in the relative proportions of the two minerals, but also by variations in magnetic grain size, the degree of aluminium substitution and degree of crystallization (e.g. Dekkers, 1989a, b; Liu et al., 2002, 2007a). In the present study, $IRM_{300\ mT}$ comprises between 3% and 20% of SIRM (Figs. 3b, 4b and 5b). Hard IRM defined by the remanence un-reversed in 100 mT comprises between 10% and 38% of SIRM. These figures are likely to underestimate the proportional contribution of the antiferromagnetic minerals by a factor between 2 and 3 orders of magnitude. Thus, even allowing for the variability documented by Liu et al. (2002, 2007a), these minerals are clearly the main components of the magnetic assemblages. Fig. 9 shows that whereas χ_{fd} values are greatly reduced in most of the samples that predate 8.5 Ma, $IRM_{300\ mT}$ values fall within roughly the same range throughout the whole of the period studied. In view of these results and the strong red coloration of the majority of the Miocene and Pliocene paleosols, there can be little doubt hematite is of major importance throughout all of the sequence.

Liu et al. (2007a) have recently proposed what they term the '*L*' ratio as a basis for establishing the extent to which the antiferromagnetic mineral assemblages are uniform in any given suite of samples. A similar index of variability in the hard remanence components can be approximated from the present data by dividing $IRM_{100\ mT}$ by $IRM_{300\ mT}$, though, as Fig. 10 shows, the use of DC rather than AF demagnetization and of $IRM_{300\ mT}$ rather than $IRM_{200\ mT}$ as the quotient gives rise to an offset in values. Where *L* values are relatively high, the overall coercivity of the antiferromagnetic assemblage is higher and vice versa. The *L* values for the whole sample set are shown in Fig. 9. The values, whether for paleosol or loess samples, decline in the upper half of the sequence with the highest values predating 14 Ma. These results confirm the limitations of $Hard_{300\ mT}$ as an indicator of antiferromagnetic concentrations and point to a long-term trend in the remanence characteristics of these minerals. This could arise from changes in the relative proportions of hematite and goethite, variations in grain size or in the degree of aluminium substitution. Although the overall trend in the *L* ratio (Fig. 9) parallels the long-term trend in global temperature inferred from $\delta^{18}O$ records in marine sediments (Zachos et al., 2001), any possible link between the two remains a matter for speculation.

5.3. The paleosol record: alternative interpretations

Following Zhou et al.'s (1990) demonstration that high χ_{lf} and χ_{fd} were associated with higher concentrations of fine viscous (FV) and SP ferrimagnetic grains resulting from pedogenesis, many studies of Quaternary loess profiles have reinforced their conclusions (e.g. Maher and Thompson, 1992; Liu et al., 1995). This has come to be regarded as typical pedogenic enhancement and has been used to define climofunctions linking soil susceptibility to both rainfall and temperature, hence to the strength and extent of summer monsoon activity (e.g. Heller et al., 1993; Maher et al., 1994; Liu et al., 1995), though some authors have noted inconsistencies in the proposed climofunctions (e.g. Guo et al., 2000, 2001a; Bloemendal and Liu, 2005).

The consistency with which, in the Pleistocene and most of the Miocene samples, higher χ_{lf} and χ_{fd} values are associated with paleosols rather than loess (Figs. 3a, 4a, 5a and 9), points to some degree of typical pedogenic enhancement. Despite the fact that variations in χ_{lf} faithfully record alternations between loess and paleosol layers on orbital timescales in most of the record, there are nevertheless strong variations from group to group not only in the peak values of χ_{lf} and χ_{fd} in paleosols, but also in most of the grain size related magnetic properties measured, as well as in the amplitude of their variations between paleosol and

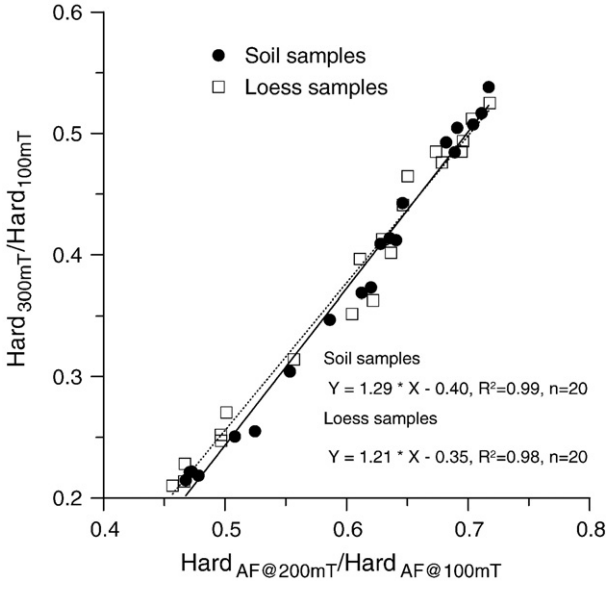

Fig. 10. Comparison between the '*L*' parameter as determined by Liu et al. (in review) and the modified version used here. $Hard_{AF@100\ mT}$ and $Hard_{AF@200\ mT}$ refer to the residual remanences after AF demagnetization of an IRM imparted in a 1 T field with a peak AF of 100 mT and 200 mT, respectively. AF demagnetization was conducted on a DTECH demagnetizer-ARM. Note the strong correlation for both loess and paleosol samples, and the consistent offset.

loess layers. Lack of a consistent trend with age casts doubt on a simple explanation in terms of long-term, time-dependent diagenesis alone. Moreover, the high carbonate content of the material and lack of evidence for waterlogging greatly reduce the likelihood of diagenesis of the magnetic minerals on supra-orbital timescales. χ_{lf} and χ_{fd} values also vary strongly from group to group in the loess layers, suggesting that the degree of 'typical' pedogenesis affecting the loess was also highly variable, though once more there is no indication of any simple long-term, time-dependent diagenetic trend.

Mass-based hard remanence measurements, whether calculated from demagnetization at −100 mT or −300 mT, fail to show similarly consistent discrimination between paleosols and loess, though there is strong evidence from elsewhere that hematite, at least in the paleosol layers, is predominantly pedogenic (Torrent et al., in press).

Two views are current regarding the ways in which fine grained ferrimagnetic minerals and hematite are produced as a result of pedogenesis. Maher and Thompson (1999) set out a scheme in terms of divergent pathways, with more moist, periodically (though not persistently) reducing conditions resulting in fine grained, non-stoichiometric magnetite (Maher, 1998; Maher et al., 2003); conversely, drier more oxidising conditions result in the direct production of hematite. Barron and Torrent (2002), on the basis of in vitro experiments, propose an alternative scheme in which maghemite is seen as the dominant, metastable, ferrimagnetic phase in a single pathway transforming paramagnetic ferrihydrite eventually into chemically stable hematite. Torrent et al. (2006, in press) outline this sequence as ferrihydrite → superparamagnetic maghemite → stable single domain maghemite → hematite. Their study also provides a convincing application of this model to the Pleistocene loess from the Luochuan section. Their results constitute strong evidence in favour of this model as the most economical for explaining the variations they find. For the present, we leave open the question of whether magnetite, maghemite or both are represented here.

Next, we consider alternative hypotheses for interpreting the possible palaeoclimatic significance of the magnetic properties of the paleosols:

1) The fine grained secondary ferrimagnets are predominantly magnetite and the 'classic' framework for interpretation of the variations in the magnetic properties of the paleosols would link peak values for χ_{lf} and χ_{fd} with maximum weathering and pedogenesis under humid/sub-humid conditions. Where hematite predominates and both χ_{lf} and χ_{fd} are relatively low, weathering under a more arid climatic regime is indicated.
2) The dominant fine grained secondary ferrimagnets are maghemite and the Torrent et al. (in press) model can be applied to the whole 22 Myr of the paleosol record. In this case, the parts of the QA profile in which both χ_{lf} and χ_{fd} are relatively low (QA_2 and QA_4), but hematite concentrations are high relative to the ferrimagnetic indicators (Fig. 5a), represent the most weathered members of the sequence and not necessarily paleosols formed under distinctively drier conditions. This hypothesis would link the paleosols with peak values for χ_{lf} and χ_{fd} to intermediate degrees of weathering without necessarily distinguishing the climatic conditions under which they formed from those prevailing when paleosols with low χ_{lf} and χ_{fd} formed. The main difference would be primarily in terms of degree of weathering and possibly soil chemistry, rather than simply climatic regime.

The present routine measurements alone do not permit conclusive resolution of these issues, though the questions raised are clearly significant, not only for the interpretation of the present data, but also for many other attempts to link the magnetic properties of paleosols to the climatic conditions under which they formed.

5.4. Magnetic evidence for weathering in the loess layers

Since the detrital input of hematite to the loess layers in the Upper Pleistocene part of the sequence at least, may have been high enough to preclude use of its changing concentrations as a weathering index (cf. Zheng et al., 1991; Chen et al., 1995), the only available indications of weathering intensity come from the χ_{lf} and χ_{fd} values (Figs. 3a, 4a, 5a and 9). On this basis, the most highly weathered loess layers come from the Dongwan section, QA_1 and possibly part of QA_3. If we assume that the small sample set from XFRE includes at least one representative of a loess layer, this too would contain indications of loess weathering under a similar weathering regime. The loess layers for which it is most difficult to make any inferences with regard to weathering are those in groups QA_2 and QA_4. Neither of the interpretative models outlined above would be inconsistent with the hematite in the QA_2+QA_4 loess layers being largely the result of weathering, though the regimes inferred would probably differ in terms of likely moisture regime. A further possibility would link variations in the magnetic properties of the loess through time to changes in weathering regimes in the source areas from which the loess came.

6. Summary and conclusions

1. The results provide the first multi-parameter magnetic measurements from pre-Pleistocene loess/paleosol sequences that began accumulation in the early Miocene. They also provide a basis for some preliminary comparisons with the more intensively studied Pleistocene sequences.
2. The degree to which the magnetic properties differentiate adjacent loess and paleosol layers varies on supra-orbital timescales. Despite this, loess–paleosol alternations are distinguishable throughout the sequence with the exception of that part of the Pliocene record represented by the *Hipparion* Red Earth (2.6–3.4 Ma). The periodicity of the alternations falls within the time-frame of orbital variability throughout the whole of the 22 Ma record.
3. The changing magnetic properties allow the record as a whole to be divided into a sequence of eight sample groups that broadly parallel the main supra-orbital changes in

magnetic susceptibility. These range from the late Pleistocene loess/paleosol couplets characterized by high amplitude variability (ca. 0.08–0.65 Ma), to late Miocene–Pliocene parts of the sequence (3.7–7 Ma) recording reduced orbital-scale variability as a result of strong weathering signatures in the loess samples, and earlier Miocene sections (8.5–14.4 Ma and 15.9–22 Ma) where loess/paleosol contrasts and longer term variability, both in ferrimagnetic concentrations and quotient values, are minimal.

4. With the exception of a brief interval from ca. 14.4 to 15.9 Ma during the Miocene, the paleosols that predate 8.5 Ma, though strongly weathered, show little indication of the formation or survival of significant amounts of pedogenic ferrimagnets; those formed after this date, irrespective of the site studied, show higher, but varying amounts of pedogenic ferrimagnets, suggesting either less complete weathering or weathering under more humid conditions, depending on the interpretational model preferred. Under the classic scheme, the Miocene periods of minimal variability, in which the ratio of fine grained ferrimagnets to antiferromagnetic minerals (predominantly hematite) is lowest, a rather arid regime would be inferred. Under the alternative scheme proposed by Torrent et al. (in press), the Miocene parts of the sequence with low ferrimagnetic concentrations could be regarded as having experienced the greatest degrees of weathering.
5. In the case of the loess layers, evidence for the weakest degree of pedogenesis comes from the Pleistocene deposits; strong evidence for weathering regimes favouring the formation and survival of pedogenic ferrimagnets are present in most samples from the period between ca. 2.6 and 8.5 Ma, spanning the Pliocene and upper Miocene. The loess layers predating this are harder to interpret in terms of weathering regimes.
6. The magnetic properties for the most part show fluctuations through time rather than any long, monotonic trends. The exception to this is the '*L*' parameter linked to changes in the coercivity of the antiferromagnetic minerals. The declining trend in *L* values through time in both loess and paleosol samples, reflecting declining coercivity, remains open to several possible interpretations pending further geochemical and rock magnetic study.
7. There is no clear evidence for long-term diagenetic alteration of the magnetic properties on timescales beyond the orbital ones that drive the loess/paleosol alternations. The geochemical context of the sites would also militate against this.
8. The present results tend to cast serious doubt on any attempt to apply existing climofunctions based on magnetic susceptibility to deposits spanning the whole of the last 22 Ma, unless more detailed rock magnetic and geochemical research provides support for the 'classic' interpretative framework from which the climofunctions have been developed.

The present study has raised more questions than it has resolved. The results of ongoing rock magnetic and geochemical studies will be presented in subsequent papers.

Acknowledgements

This study was supported by the Chinese Academy of Sciences (KZCX2-YW-117), 973 project 2004CB720203, and the National Natural Science Foundation of China (projects 40672115 and 40730104). J. Bloemendal and Q. Hao thank the Royal Society for financial support. We are grateful to Mr. Bob Jude for the measurement of routine magnetic property and to Professors Jose Torrent, Vidal Barron and Dr. Qingsong Liu for helpful discussions.

References

An, Z.S., Kukla, G., Porter, S.C., Xiao, J.L., 1991. Magnetic susceptibility evidence of monsoon variation on the Loess Plateau of central China during the last 130,000 years. Quaternary Research 36, 29–36.

Banerjee, S.K., King, J., Marvin, J., 1981. A rapid method for magnetic granulometry with applications to environmental studies. Geophysical Research Letters 20, 333–336.

Barron, V., Torrent, J., 2002. Evidence for a simple pathway to maghemite in Earth and Mars soils. Geochimica et Cosmochimica Acta 66, 2801–2806.

Belbin, L., 1987. PATN (Pattern Analysis Package). Reference Manual. CSIRO Division of Wildlife and Rangelands Research, Canberra.

Belbin, L., 1988. PATN pattern analysis package. Users guide. Commonwealth Scientific and Industrial Research Organization, Australia.

Bloemendal, J., Liu, X., 2005. Rock magnetism and geochemistry of two Plio-Pleistocene Chinese loess–palaeosol sequences—implications for quantitative palaeoprecipitation reconstructions. Palaeogeography, Palaeoclimatology, Palaeoecology 226, 149–166.

Chen, F.H., Wu, R.J., Pompei, D., Oldfield, F., 1995. Magnetic property and particle size variations in the late Pleistocene and Holocene parts of the Dadongling loess section near Xining, China. Quaternary Proceedings 4, 27–40.

Dearing, J.A., Dann, R.J.L., Hay, K., Lees, J.A., Loveland, P.J., Maher, B.A., O'Grady, K., 1996. Frequency dependent susceptibility measurements of environmental materials. Geophysical Journal International 124, 228–240.

Dekkers, M.J., 1989a. Magnetic properties of natural goethite—I. Grain-size dependence of some low- and high-field related rockmagnetic parameters measured at room temperature. Geophysical Journal International 97, 323–340.

Dekkers, M.J., 1989b. Magnetic properties of nature goethite—II. TRM behaviour during thermal and alternating field demagnetization and low-temperature treatment. Geophysical Journal International 97, 341–355.

Evans, M.E., Heller, F., 2001. Magnetism of loess/palaeosol sequences: recent developments. Earth-Science Reviews 54, 129–144.

Evans, M.E., Heller, F., 2003. Environmental Magnetism. Academic Press, New York.

Guo, Z.T., Biscaye, P., Wei, X., Chen, X., Peng, S., Liu, T., 2000. Summer monsoon variations over the last 1.2 Ma from the weathering of loess–soil sequences in China. Geophysical Research Letters 27, 1751–1754.

Guo, B., Zhu, R.X., Roberts, A.P., Florindo, F., 2001a. Lack of correlation between paleoprecipitation and magnetic susceptibility of Chinese loess/palaeosol sequences. Geophysical Research Letters 28, 4259–4262.

Guo, Z.T., Peng, S.Z., Hao, Q.Z., Biscaye, P.E., Liu, T.S., 2001b. Origin of the Miocene–Pliocene Red-Earth formation at Xifeng in Northern China and implications for paleoenvironments. Palaeogeography, Palaeoclimatology, Palaeoecology 170, 11–26.

Guo, Z.T., Ruddiman, W.F., Hao, Q.Z., Wu, H.B., Qiao, Y.S., Zhu, R.X., Peng, S.Z., Wei, J.J., Yuan, B.Y., Liu, T.S., 2002. Onset of Asian desertification by 22 Myr ago inferred from loess deposits in China. Nature 416, 159–163.

Guo, Z.T., Hao, Q.Z., Wei, J.J., An, Z.S., 2004a. Astronomical signals in different climate proxies from the Quaternary loess/soil sequences in China. Milutin Milankovitch Anniversary Symposium: Paleoclimate and Earth System Climate. Serbian Academy of Sciencess, Belgrade, pp. 95–105.

Guo, Z.T., Peng, S.Z., Hao, Q.Z., Biscaye, P., An, Z.S., Liu, T.S., 2004b. Late Miocene–Pliocene development of Asian aridification as recorded in the

Red-Earth Formation in northern China. Global and Planetary Change 41, 135–145.
Han, J.M., Lü, H.Y., Wu, N.Q., Guo, Z.T., 1996. The magnetic susceptibility of modern soils in China and its use for paleoclimate reconstruction. Studia Geophysica et Geodaetica 40, 262–275.
Hao, Q.Z., Guo, Z.T., 2004. Magnetostratigraphy of a late Miocene–Pliocene loess–soil sequence in the western Loess Plateau in China. Geophysical Research Letters 31, L092099. doi:10.1029/2003GL019392.
Hao, Q.Z., Guo, Z.T., 2005. Spatial variations of magnetic susceptibility of Chinese loess for the last 600 kyr: implications for monsoon evolution. Journal of Geophysical Research 110, B12101. doi:10.1029/2005BJ003765.
Heller, F., Liu, T.S., 1984. Magnetism of Chinese loess deposits. Geophysical Journal of the Royal Astronomical Society 77, 125–141.
Heller, F., Evans, M.E., 1995. Loess magnetism. Reviews of Geophysics 33, 211–240.
Heller, F., Shen, C.D., Beer, J., Liu, X.M., Liu, T.S., Bronger, A., Suter, M., Bonani, G., 1993. Quantitative estimates of pedogenic ferromagnetic mineral formation in Chinese loess and palaeoclimatic implications. Earth and Planetary Science Letters 114, 385–390.
Li, F.J., Wu, N.Q., Pei, Y.P., Hao, Q.Z., Rousseau, D.-D., 2006a. Wind-blown origin of Dongwan late Miocene–Pliocene dust sequence documented by land snail record in western Chinese Loess Plateau. Geology 34, 405–408. doi:10.1130/G22232.1.
Li, F.J., Wu, N.Q., Rousseau, D.-D., 2006b. Preliminary study of mollusk fossils in the Qinan Miocene loess–soil sequence in western Chinese Loess Plateau. Science in China. Series D: Earth Sciences 49, 724–730.
Liu, Q.S., Banerjee, S., Jackson, M.J., 2002. A new method in mineral magnetism for the separation of weak antiferromagnetic signal from strong ferrimagnetic background. Geophysical Research Letters 29. doi:10.1029/2002GL014699.
Liu, X.M., Rolph, T., Bloemendal, J., Shaw, J., Liu, T.S., 1995. Quantitative estimates of palaeoprecipitation at Xifeng, in the Loess Plateau of China. Palaeogeography, Palaeoclimatology, Palaeoecology 13, 243–248.
Liu, X.M., Rolph, T., An, Z.S., Hesse, P., 2003. Paleoclimatic significance of magnetic properties on the Red Clay underlying the loess and paleosols in China. Palaeogeography, Palaeoclimatology, Palaeoecology 199, 153–166.
Liu, Q.S., Banerjee, S.K., Jackson, M.J., Deng, C., Pan, Y., Zhu, R., 2004a. New insights into partial oxidation model of magnetites and thermal alteration of magnetic mineralogy of the Chinese loess in air. Geophysical Journal International 158, 506–514.
Liu, Q.S., Jackson, M.J., Yu, Y.J., Chen, F.H., Deng, C.L., Zhu, R.X., 2004b. Grain size distribution of pedogenic magnetic particles in Chinese loess/paleosols. Geophysical Research Letters 31, L22603. doi:10.1029/2004GL021090.
Liu, J.F., Guo, Z.T., Hao, Q.Z., Peng, S.Z., Qiao, Y.S., Sun, B., Ge, J.Y., 2005. Magnetostratigraphy of the Miziwan Miocene aeolian deposits in Qinan County (Gansu Province) (in Chinese with an English abstract). Quaternary Sciences 25, 503–509.
Liu, J.F., Guo, Z.T., Qiao, Y.S., Hao, Q.Z., Yuan, B.Y., 2006. Eaolian origin of the Miocene loess–soil sequence at Qin'an, China: evidence of quartz morphology and quartz grain-size. Chinese Science Bulletin 51, 117–120.
Liu, Q.S., Robert, A.P., Torrent, J., Horng, C., Larrasoana, J.C., 2007a. What do the HIRM and S-ratio parameters really measure in environmental magnetism? Geochemistry Geophysics Geosystems 8, Q09011. doi:10.1029/2007GC001717.
Liu, Q., Deng, C., Torrent, J., Zhu, R., 2007b. Review of recent developments in mineral magnetism of the Chinese loess. Quaternary Science Reviews 26, 368–385.
Maher, B., 1988. Magnetic properties of some sub-micron synthetic magnetites. Geophysical Journal 94, 83–96.
Maher, B.A., 1998. Magnetic properties of modern soils and Quaternary loessic palaeosols: palaeoclimatic implications. Palaeogeography, Palaeoclimatology, Palaeoecology 137, 25–54.
Maher, B.A., Thompson, R., 1992. Palaeoclimatic significance of the mineral magnetic record of Chinese loess and palaeosols. Quaternary Research 37, 155–170.
Maher, B.A., Thompson, R., 1999. Palaeomonsoons I: the magnetic record of palaeoclimate in the terrestrial loess and palaeosol sequences. In: Maher, B.A., Thompson, R. (Eds.), Quaternary Climates, Environments and Magnetism. Cambridge University Press, Cambridge, pp. 81–125.
Maher, B.A., Thompson, R., Zhou, L.P., 1994. Spatial and temporal reconstructions of changes in the Asian palaeomonsoon — a new mineral magnetic approach. Earth and Planetary Science Letters 125, 461–471.
Maher, B.A., Alekseev, A., Alekseeva, T., 2003. Magnetic mineralogy of soils across the Russian Steppe: climatic dependence of pedogenic magnetite formation. Palaeogeography, Palaeoclimatology, Palaeoecology 201, 321–341.
Oldfield, F., 1994. Toward the discrimination of fine grained ferrimagnets by magnetic measurements in lake and near-shore marine sediments. Journal of Geophysical Research 99, 9045–9050.
Oldfield, F., in press. Sources of fine grained magnetic minerals in sediments: a problem revisited. The Holocene.
Oldfield, F., Crowther, J., 2007. Establishing fire incidence in temperate soils using magnetic measurements. Palaeogeography, Palaeoclimatology, Palaeoecology 249, 362–369.
Oldfield, F., Wake, R., Boyle, J., Jones, R., Nolan, S., Gibbs, Z., Appleby, P.G., Fisher, E., Wolff, G., 2003. The Late-Holocene history of Gormire Lake (N.E. England) and its catchment: a multi-proxy reconstruction of past human impact. The Holocene 13, 677–690.
Qiao, Y.S., Guo, Z.T., Hao, Q.Z., Yin, Q.Z., Yuan, B.Y., Liu, T.S., 2006. Grain-size features of a Miocene loess–soil sequence at Qinan: implications on its origin. Science in China, Series D: Earth Sciences 49, 731–738.
Thompson, R., Oldfield, F., 1986. Environmental Magnetism. Allen and Union, London.
Torrent, J., Barrón, V., Liu, Q.S., 2006. Magnetic enhancement is linked to and precedes hematite formation in aerobic soil. Geophyscal Research Letters 33, L02401. doi:10.1029/2005GL024818.
Torrent, J., Liu, Q., Bloemendal, J., in press. Effects of pedogenesis on magnetic properties of the loess/paleosol sequences from the upper Luochuan section, central China Loess Plateau. Earth and Planetary Science letters.
Walden, J., Oldfield, F., Smith, J. (Eds.), 1999. Environmental Magnetism: a Practical Guide. Technical Guide No. 6. Quaternary Research Association, London.
Yu, L., Oldfield, F., 1993. Quantitative sediment source ascription using magnetic measurements in a reservoir–catchment system near Nijar, S.E. Spain. Earth Surface Processes and Landforms 18, 441–454.
Zachos, J., Pagani, M., Sloan, L., Thomas, E., Billups, K., 2001. Trends, rhythms and aberrations in global climate 65 Ma to present. Science 292, 686–693.
Zheng, H., Oldfield, F., Yu, L., Shaw, J., An, Z., 1991. The magnetic properties of particle-sized samples from the Luo Chuan loess section: evidence for pedogenesis. Physic of the Earth and Planetary Interiors 68, 250–258.
Zhou, L.P., Oldfield, F., Wintle, A.G., Robinson, S.G., Wang, J.T., 1990. Partly pedogenic origin of magnetic variations in Chinese loess. Nature 346, 737–739.